Isolation and Characterization of a Monoclonal Anti-Quadruplex DNA Antibody from Autoimmune "Viable Motheaten" Mice[†,‡]

Bernard A. Brown, II,[§,||] Yangqi Li,[§] Julie C. Brown,[§,⊥] Charles C. Hardin,[*,§] John F. Roberts,[▽] Stephen C. Pelsue,[○,∞] and Leonard D. Shultz[○]

Departments of Biochemistry and Zoology, North Carolina State University, Raleigh, North Carolina 27695, and The Jackson Laboratory, Bar Harbor, Maine 04069

Received June 9, 1998; Revised Manuscript Received August 26, 1998

ABSTRACT: A cell line that produces an autoantibody specific for DNA quadruplex structures has been isolated and cloned from a hybridoma library derived from 3-month-old nonimmunized autoimmune, immunodeficient "viable motheaten" mice. This antibody has been tested extensively in vitro and found to bind specifically to DNA quadruplex structures formed by two biologically relevant sequence motifs. Scatchard and nonlinear regression analyses using both one- and two-site models were used to derive association constants for the antibody−DNA binding reactions. In both cases, quadruplexes had higher association constants than triplex and duplex molecules. The anti-quadruplex antibody binds to the quadruplex formed by the promoter-region-derived oligonucleotide d(CGCG$_4$GCG) ($K_a = 3.3 \times 10^6$ M^{-1}), and has enhanced affinity for telomere-derived quadruplexes formed by the oligonucleotides d(TG$_4$) and d(T$_2$G$_4$T$_2$G$_4$T$_2$G$_4$T$_2$G$_4$) ($K_a = 5.38 \times 10^6$ and 1.66×10^7 M^{-1}, respectively). The antibody binds both types of quadruplexes but has preferential affinity for the parallel four-stranded structure. In vitro radioimmunofilter binding experiments demonstrated that purified anti-DNA quadruplex antibodies from anti-quadruplex antibody-producing tissue culture supernatants have at least 10-fold higher affinity for quadruplexes than for triplex and duplex DNA structures of similar base composition and length. The antibody binds intramolecular DNA triplexes formed by d(G$_4$T$_3$G$_4$T$_3$C$_4$) and d(C$_4$T$_3$G$_4$T$_3$G$_4$), and the duplex d(CGCGCGCGCG)$_2$ with an affinities of 6.76×10^5, 5.59×10^5, and 8.26×10^5 M^{-1}, respectively. Competition experiments showed that melted quadruplexes are not effective competitors for antibody binding when compared to native structures, confirming that the quadruplex is bound structure-specifically. To our knowledge, this is the first immunological reagent known to specifically recognize quadruplex structures. Subsequent sequence analysis demonstrates homologies between the antibody complementarity determining regions and sequences from Myb family telomere binding proteins, which are hypothesized to control cell aging via telomeric DNA interactions. The presence of this antibody in the autoimmune repertoire suggests a possible linkage between autoimmunity, telomeric DNA binding proteins, and aging.

Guanine-rich DNA sequences can form a variety of four-stranded structures containing G·G base pairs that are stabilized by physiologically important cations such as K^+ and Na^+ (for reviews see refs *1*−*4*). G-rich DNA fragments derived from at least three discrete regions in eukaryotic genomes, telomeres, immunoglobulin-switching regions, and transcriptional promoters, can form quadruplexes (see refs *4* and *5*). A number of quadruplex conformational variants have been described and several biological roles have been suggested in telomere−telomere fusions, telomerase inhibition, chromatin condensation, mitotic and meiotic pairing, promotion of recombination, and repression of transcription and replication (*4*, *6*−*16*). Quadruplexes may also play a role in the recognition of eukaryotic intron RNA by A1 heterogeneous nuclear ribonucleoprotein (hnRNP) (*17*).

Chromosomal abnormalities have been linked to G-rich quadruplex DNAs. Fragile X syndrome is associated with contiguous d(CGG)$_n$ trinucleotide repeats, which have been shown to form stable quadruplexes in vitro (*18*). This is an important disease because it is responsible for developmentally mediated mental retardation in ca. 1 out of 2000 humans. Other quadruplex-prone sequences include recognition sites for the proteins MyoD, RAP1, c-Ha-*ras*, and the SP1 transcription factor (*5*, *19*−*24*). Quadruplexes derived from immunoglobulin switch region DNAs bind specifically to the *QUAD* protein from rabbit hepatocytes (*25*). Despite

[†] Supported by grants to C.C.H. from National Institutes of Health (GM47431), North Carolina Biotechnology Center, and North Carolina Agricultural Research Service. Work at The Jackson Laboratory was supported by National Institutes of Health Grants CA20408 (L.D.S.) and DK07449 (S.C.P.).

[‡] This report was presented in preliminary form at the Symposium on RNA Biology, Research Triangle Park, NC, October 13−15, 1995; *Nucleic Acids Res. Symp. Ser. 33*, 134−136.

* To whom correspondence should be addressed.

[§] Department of Biochemistry, NC State.

[||] Present address: Department of Biology, Massachusetts Institute of Technology, Cambridge, MA 02139.

[⊥] Present address: Large Scale Molecular Biology Laboratory, Genetics Institute, 87 Cambridge Park Dr., Cambridge, MA 02140.

[▽] Department of Zoology, NC State.

[○] The Jackson Laboratory.

[∞] Present address: Department of Applied Immunology, University of Southern Maine, 117 Science Building P.O. Box 9300, Portland, ME 04103.

10.1021/bi981354u CCC: $15.00
Published on Web 10/29/1998

these interesting correlations, quadruplexes have eluded definitive detection in vivo thus far.

Antibodies can be used to elucidate structural features of native and modified nucleic acids and their complexes. Right- and left-handed DNAs and RNAs and triple-helical DNAs have all been studied in vitro and in vivo by using poly- and monoclonal antibodies (*26*−*47*). In another example, bent DNA was detected immunochemically in the kinetoplast DNA of the parasite *Leishmania tarentolae* (*41*, *48*).

Many different anti-DNA antibodies have been obtained from murine models of systemic lupus erythematosus. Specifically, (NZB × NZW) F_1 and MRL/Mp-*lpr*/*lpr* mice have been shown to produce antibodies that are specific for single- and double-stranded DNA, Z-DNA, RNA, and rRNA (*27*, *35*, *42*, *44*, *47*, *49*−*59*).

The key to characterizing a truly useful anti-quadruplex immunoreagent is knowing the specific affinity of the antibody and its selectivity relative to other nucleic acid conformations that might be encountered during use. The properties of a promising specific anti-quadruplex antibody are described here.

EXPERIMENTAL PROCEDURES

Production and Purification of Synthetic DNAs. The oligonucleotides d(CGCG$_4$GCG), d(TG$_4$), d(T$_2$G$_4$T$_2$G$_4$T$_2$G$_4$T$_2$G$_4$), d(G$_4$T$_3$G$_4$T$_3$C$_4$), d(C$_4$T$_3$G$_4$T$_3$G$_4$), and d(CGCGCGCGCG) were synthesized at the NCSU Molecular Genetics Facility by standard β-cyanoethyl phosphoramidite chemistry on an Applied Biosystems DNA/RNA synthesizer. Reaction products were eluted from the silica solid support in concentrated NH_4OH and then lyophilized to dryness and dialyzed against 200 mM KCl, to stabilize quadruplexes, or 200 mM NaCl, to prepare the other complexes. Samples were lyophilized again and dialyzed extensively against 0.1 mM K_2EDTA[1] (pH 7) or 0.1 mM Na_2EDTA (pH 7) and stored for use at 4 °C. Hydrolyzed herring sperm DNA was purchased from Sigma and sonicated calf thymus DNA was purchased from Pharmacia; both were resuspended in TES buffer containing 50 mM Tris·HCl (pH 7.4), 1 mM EDTA, and 50 mM NaCl. Concentrations were determined from UV absorbances measured at 260 nm and molar extinction coefficients that were calculated for single strands based on the nearest-neighbor approximation using the program OLIGO 4.0 (National Biosciences, Inc.). Sample purity and integrity were verified by nuclear magnetic resonance (NMR), circular dichroism (CD), and gel electrophoretic analyses.

Radiolabeled DNAs were prepared with T4 polynucleotide kinase and [γ-^{32}P]ATP according to the manufacturer's instructions (Promega). Labeled DNAs were purified from unincorporated [γ-^{32}P] ATP using NENsorb20 nucleic acid purification cartridges (New England Nuclear) or G-25 spin columns (5′ → 3′ or Boehringer-Mannheim). Labeled stocks were quantitated by UV absorbance as described above and were stored at −20 °C in TES buffer.

Circular dichroism analyses were performed by diluting stock solutions to ca. 7 μM in 10 mM NaH_2PO_4 buffer (pH 7) in a volume of 1 mL. Spectra in the wavelength range 210−350 nm were acquired on a Jasco J-600 spectropolarimeter at 25 °C as described previously (*5*, *60*, *61*). Thermal denaturation data were obtained in a 1 cm water-jacketed CD cell that was equilibrated to the appropriate temperature. Denaturation of quadruplexes to produce single strands was performed by incubating the samples for 1 h at 100 °C in 0.1 mM Li_2EDTA buffer (pH 7) and then allowing them to cool to 25 °C.

^{1}H NMR analyses were performed on a GE 500 MHz spectrometer at 25 °C with 5 mM DNA samples (in strands) in 10 mM NaH_2PO_4 buffer (pH 7) containing 10% D_2O; sample volumes were 500 μL. The 1−1 hard pulse solvent suppression technique or presaturation were used to reduce the HDO resonance (*62*). Typically, 512 scans were obtained in 8K data sets at a spectral width of 10 000 Hz; deuterated sodium 3-(trimethylsilyl)-1-propanesulfonic acid (TSP) was used as internal chemical shift reference. Characteristic quadruplex amino and imino resonances in the 6.5−12 ppm range (data not shown) verified that these oligonucleotides formed the appropriate structures (*4*, *6*, *60*).

Preparation of Viable Motheaten Hybridomas. Hybridomas were produced from autoimmune, immunodeficient "viable motheaten" mice (C57BL/6J-*Hcph*$^{me-v}$/*Hcph*$^{me-v}$). Two 3-month-old viable motheaten mice were obtained from the Jackson Laboratory (Bar Harbor, ME) and were maintained about 2 weeks after arrival in a sterile isolator cage and fed autoclaved food and water ad libitum. Mice were not immunized prior to lymphectomy. On the night prior to performing fusions, the mice were injected with 20−50 μL of sterile 1% Evans Blue subcutaneously in the cervical region and intraperitoneally. Macrophages and polymorphonuclear lympocytes sequester the dye in the lymphoid organs, allowing easy identification during lymphectomy. Cells isolated from the lymph nodes (axiliary, brachial, cervical, inguinal, mesenteric, and popliteal) were fused with non-Ig-secreting P3 × 63Ag8.653 myeloma cells at a 1:1.5 lymphocyte:myeloma ratio with poly(ethylene glycol) 1500 (Boehringer-Mannheim) according to standard fusion procedures (*63*). Fusions of the lymph nodes from each mouse were performed separately. Afterward, cells were dispensed into 24-well tissue culture plates, selected in HAT medium (RPMI-1640 medium containing 100 μM hypoxanthine, 0.4 μM aminopterin, 16 μM thymidine, 2 mM glutamine, 1% glucose, 10% FBS, 100 units/mL penicillin, 100 μg/mL streptomycin, 2.5 μg/mL amphotericin, and 50 μg/mL gentamycin) for 12 days, and then switched to HT medium (HAT medium without aminopterin) for 10 days. Surviving hybridomas were maintained in RPMI-1640 medium supplemented with 2 mM glutamine, 5−10% FBS, and antibiotics at 37 °C in a humidified incubator under air and 5% CO_2.

Production and Screening of a Viable Motheaten Hybridoma Library. A cellular library of hybridomas from viable motheaten mice was generated by combining the surviving

[1] Abbreviations: CD, circular dichroism; C-RIFB, competitive radioimmunofilter binding; CG5, self-complementary intermolecular duplex formed by d(CGCGCGCGCG); EDTA, ethylenediaminetetracetic acid; G4, parallel-stranded quadruplex formed by d(CGCG$_4$GCG); Ig, immunoglobulin; FBS, fetal bovine sera; NMR, nuclear magnetic resonance; Q, quadruplex; RIFB, radioimmunofilter binding; TBS, Tris-buffered saline, containing 25 mM Tris·HCl (pH 7.4), 137 mM NaCl, and 2.7 mM KCl; TES, 25 mM Tris·HCl (pH 7.4), 10 mM EDTA, and 50 mM NaCl; TET4, d(T$_2$G$_4$T$_2$G$_4$T$_2$G$_4$T$_2$G$_4$), which can form a single-stranded intramolecular antiparallel quadruplex, a bimolecular quadruplex composed of two hairpins, and a parallel-stranded tetramolecular quadruplex; TG4, parallel-stranded quadruplex formed by d(TG$_4$); Tris·HCl, tris(hydroxymethyl)aminomethane hydrochloride.

hybridomas and propagating the cells as a mixed culture. Cells were collected from plates and flasks approximately every 3 days and centrifuged at 5000 rpm for 10 min. The supernatant was discarded and the cells were resuspended in 82% FCS, 10% RPMI medium, and 8% DMSO and slowly frozen (≈1 °C/min) in a −80 °C freezer before being transferred to a liquid N_2 dewar. A "master" library was produced by combining the sublibraries and then propagating them as a single culture. No screenings for antigen reactivity were performed during this phase of culturing.

Screenings for antibody-binding activity to nucleic acid substrates were accomplished by diluting frozen stocks of each sublibrary or the master library in RPMI medium and dispensing into 24-well culture plates. Cell cultures were grown for 2−3 days and then screened for reactivity to specific nucleic acid structures. Binding activity was detected by removing 1 mL of medium from each individual culture (usually prior to feeding) and subjecting it to radioimmunofilter binding (RIFB) assays with each nucleic acid of interest. Cultures that exhibited positive binding activity were expanded and propagated in 25 and 75 cm^2 tissue culture flasks. Monoclonal hybridomas were obtained by sequential limiting dilution cloning. Frozen stocks of ca. 10^6 cells were frozen and stored in liquid N_2 as described above.

Production and Purification of Anti-DNA Quadruplex Antibodies. Hybridomas were grown for large-scale production of antibodies in 1 L Corning slow speed stirring vessels in RPMI medium supplemented with 10 mM HEPES (pH 7.4) and 5% FBS under air at 37 °C with continuous stirring. Cultures were maintained until the medium turned bright yellow and cell viability was negligible as determined by trypan blue exclusion. Cells were pelleted by centrifugation at 3000*g* for 10 min and discarded.

Antibodies from the tissue culture supernatants were concentrated by ammonium sulfate precipitation then purified by gel-filtration chromatography on a Sephacryl 400 HR column (Pharmacia) in 50 mM NaH_2PO_4 (pH 7.4) and 100 mM NaCl at room temperature. Fractions were collected and the elution absorbance profile was monitored at 280 and 254 nm. Individual fractions from absorbance peaks were assayed for the presence of antibodies by ELISA using goat anti-mouse Ig(G, M, A)−alkaline phosphatase immunoconjugates (Sigma) according to standard protocols (*64*). The gel−filtration chromatography method did not yield pure products as determined by SDS−PAGE. Therefore, several alternative chromatographic resins were tested in attempts to achieve higher purity of the antibody. These included heparin−cellulose (Gibco−BRL Life Sciences), Sepharose-Cibacron Blue (Pharmacia), phosphocellulose (Whatman), and Sepharose DEAE (Pharmacia). Thiophilic T-Gel resin (Pierce) was chosen as the most effective method of purification.

Tissue culture supernatants containing antibodies were grown in large-scale cultures and cells were pelleted as described above. The supernatant was neutralized by the addition of 1 M Tris·HCl (pH 8) to achieve a final concentration of 10 mM, and then solid K_2SO_4 was added to produce a 0.5 M K_2SO_4 solution (87 mg of K_2SO_4/mL of supernatant). The solution was stirred gently for 10 min to dissolve the K_2SO_4 and then centrifuged at 10000*g* for 20 min to pellet any precipitant. The supernatant solution was removed and then loaded on a 1 mL T-Gel column at a flow rate of ≈100 μL/min. The column was washed with 10 volumes of 0.5 M K_2SO_4 in 50 mM Tris·HCl (pH 8) and then the antibody sample was eluted with 5 mL of 50 mM Tris·HCl (pH 8). The column was regenerated with 8 M guanidine hydrochloride and stored at 4 °C in 50 mM Tris·HCl (pH 8) containing 0.02% NaN_3 between uses. The antibody eluate was detected by monitoring the elution absorbance profiles at 280 and 254 nm. ELISA was used to confirm that the eluted peak contained the purified antibody as described above. Following purification, antibody samples were concentrated with Centricon or CentriPrep concentrators (Amicon). Protein concentrations were determined by the bicinchoninic acid (BCA) protein assay (Pierce).

Anti-DNA quadruplex antibodies were isotyped by use of an ELISA clonotyping system, which involves characterization by isotype-specific antibodies (Southern Biotechnology Associates). Antibody samples were compared to IgM, IgG1, IgG2a, IgG2b, IgG3, and IgA standards. PCR-based genetic isotyping was performed with the Ig-Prime kit according to the instructions provided by the manufacturer (Novagen). Primers for IgM, IgG1, IgG2a, IgG2b, and IgG3 heavy chains and κ and λ light chains were tested. Purified antibody stocks were stored in TBS containing 0.02% NaN_3 at 4 °C for short-term storage or −20 °C for long-term storage. Samples were also dialyzed into TES buffer for some RIFB assays.

Purities of antibody samples were determined by sodium dodecyl sulfate−polyacrylamide gel electrophoresis (SDS−PAGE). Antibody preparations were incubated for 15 min at 100 °C in reducing loading dye [375 mM Tris·HCl (pH 8.8), 20% glycerol, 4% SDS, 285 mM 2-mercaptoethanol, and 1% bromophenol blue], and then loaded onto 6% or 8% polyacrylamide minigels [375 mM Tris·HCl (pH 8.8) and 0.1% SDS] and electrophoresed in running buffer [25 mM Tris·HCl (pH 8.3), 192 mM glycine, and 0.1% SDS] for 1 h at 100 V (12 V/cm). Gels were stained with Coomassie blue and then destained in 5% (v/v) methanol and 7% (v/v) acetic acid to visualize the bands.

Alternatively, electrophoretically resolved antibody bands were transferred to nitrocellulose membranes for Western analysis with a Mighty Small Transphor electroblotter (Hoefer) in transfer buffer [25 mM Tris·HCl (pH 8.3), 192 mM glycine, and 20% methanol] operating at 100 V for 1.5 h (*65*). Nonspecific protein binding was blocked with 10% horse serum in TBS for 2 h, and then the blot was washed twice with TBST (TBS containing 0.05% Tween 20) and finally again with TBS. Blots were probed with goat anti-mouse Ig−alkaline phosphatase immunoconjugates that are specific for individual mouse immunoglobulin isotypes (Southern Biotechnology Associates; diluted 1:1000 in TBS containing 5% BSA) and developed with 3-bromo-4-chloro-3-indolyl phosphate/nitro blue tetrazolium (BCIP/NBT).

Immunochemical Assays. RIFB assays were performed to detect antibody binding activity by modifying procedures of Möller et al. (*31*) and Hardin et al. (*36*). Tissue culture supernatants or purified antibodies (≈25 μM) were incubated for 2 h at 37 °C in sterile siliconized 0.5 mL microcentrifuge tubes with 0−1 mmol of ^{32}P-end-labeled DNA substrates in TES buffer in a total volume of 100 μL. Anti-DNA IgM (Boehringer-Mannheim) was used as a positive control for

double-stranded DNA binding. Sera that were specific for double- and single-stranded DNAs from autoimmune MRL/Mp-*lpr*/*lpr* mice were generously donated by Drs. Elizabeth Reap and Phil Cohen (Department of Rheumatology, University of North Carolina, Chapel Hill) for use as positive controls for anti-DNA binding activity. Native and denatured calf thymus or herring sperm DNA were prepared as described by Zouali and Stollar (*66*) and were used in the control assays. Following incubation, reactions were transferred to individual wells of MultiScreen-HA 0.45 μm nitrocellulose microtiter filtration plates (Millipore) that had been presoaked with TBS. Reactions were incubated in the plate for 10 min at 25 °C, aspirated through filters that were washed once with TBST and then four times with TBS, and air-dried at room temperature for 30 min. Individual filters were punched into vials, suspended in 1 mL of scintillation cocktail, and counted by liquid scintillation.

Substrate Binding Assays. Binding isotherms were obtained from RIFB assays, which measured DNA−antibody binding as a function of DNA concentration at a single antibody concentration. Radiolabeled DNA quadruplexes or other substrates (0−100 μmol) were incubated in TES with a constant amount of purified *me*$^{\nu}$IIB4 antibody (≈25 μM in TBS) for 2 h at 37 °C in a total volume of 100 μL. The amount of radiolabeled DNA in each sample was determined by placing each 0.5 mL reaction tube within a 5 mL glass scintillation vial and counting by scintillation during the incubation period. After incubation, each reaction was transferred to an individual well of a Multiscreen-HA filtration plate and processed as described above. Individual filters were punched and counted by liquid scintillation. Background binding values of radiolabeled DNAs to the filter (without antibody present) were subtracted from the measured "bound" values. Assays were repeated at least twice and mean scintillation values were calculated.

The concentration of DNA bound by the antibody on the nitrocellulose filters (C_{bound}) was calculated from

$$C_{bound} = \frac{cpm_{bound} C_{total}}{cpm_{total}} \quad (1)$$

where cpm_{bound} is the counts per minute (cpm) of the DNA bound to the antibody, cpm_{total} is the total cpm of DNA in each sample (measured during the incubation period), and C_{total} is the total DNA concentration in the reaction. The concentration of unbound DNA (C_{free}) was calculated from

$$C_{free} = C_{total} - C_{bound} \quad (2)$$

where C_{total} is the total DNA concentration and C_{bound} is the concentration bound to the antibody (after subtraction of background DNA bound to the nitrocellulose filter).

The binding function, *r*, (also termed ν; *67*) is defined as the molar ratio of bound DNA to the total concentration of antibody sites, C_s (C_s = twice the total molar IgG3 concentration) as shown:

$$r = C_{bound}/C_s \quad (3)$$

The value of *r* represents specific binding, the amounts of ligand (DNA) bound *per* Fab *site*, not bound ligand.

Binding data were analyzed by plotting the transformed results as r/C_{free} vs *r* (*67*). Binding parameters were obtained from linear Scatchard plots according to

$$r/C_{free} = K_a(n - r) \quad (4)$$

where *r* is the binding function, C_{free} is the free DNA concentration, K_a is the DNA−antibody binding site equilibrium association constant, and *n* (the *x*-intercept) is the maximum concentration of binding sites. Since all substrates used in the binding assays are monovalent (i.e., they can only be bound by *one* Fab *site* at a time), then we can assume that each Fab site binds a single ligand (under saturating ligand concentrations). Thus, *n* is equal to the molar concentration of ligands bound by each Fab site. *This assumption is only legitimate because each* Fab *site is treated in isolation and all substrates are monovalent.*

Binding data were also plotted as the binding function versus the concentration of free DNA (*r* vs C_{free}) and analyzed by nonlinear regression using the program PRISM 2.0 (GraphPad Software, Inc.). The PRISM program fits the one-site rectangular hyperbolic binding isotherm according to

$$r = \frac{B_{max} C_{free}}{K_d + C_{free}} \quad (5)$$

where *r* is the binding function, B_{max} is the total concentration of binding sites ($B_{max} = n$, as described above), C_{free} is the free DNA concentration, and K_d is the DNA−antibody equilibrium dissociation constant (*68*, *69*).

A third method that was used to analyze antibody-DNA binding data involved treating the antibody molecule as a multivalent macromolecule with *two linked sites* (i.e., cooperativity is relevant). In this case, binding of a ligand to one site can affect subsequent ligand binding to the other site. Binding data were fit to the two-site model by both linear and nonlinear regression analyses using PRISM 2.0 (GraphPad Software, Inc.). In these analyses, the actual concentration of the antibody was used, instead of the concentration of antigen-binding sites.

The hyperbolic upward-curved Scatchard plots can be decomposed into two components, which correspond to the linear Scatchard plots of the separate affinities of each binding site (i.e., one high binding affinity component and another lower binding affinity component). The two-binding-site Scatchard plot can be described by

$$r/C_{free} = \frac{n_1 K_{d_1}}{1 + K_{d_1} C_{free}} + \frac{n_2 K_{d_2}}{1 + K_{d_2} C_{free}} \quad (6)$$

where *r* is the binding function, C_{free} is the free DNA concentration, K_d is the DNA−antibody binding site equilibrium association constant, and *n* (the *x*-intercepts) are the concentrations of binding sites.

The final method utilized to analyze binding data was a two-site nonlinear regression method calculated by the program PRISM 2.0 (GraphPad Software, Inc.). The PRISM program fitted the two-site rectangular hyperbolic binding isotherm according to

$$r = \frac{B_{max_1} C_{free}}{K_{d_1} + C_{free}} + \frac{B_{max_2} C_{free}}{K_{d_2} + C_{free}} \quad (7)$$

where r is the binding function, B_{max1} and B_{max2} are the individual concentrations of binding sites ($B_{max} = n$, as described above), C_{free} are the free DNA concentrations, and K_d are the DNA−antibody equilibrium dissociation constants (*68*, *69*).

Anti-DNA Quadruplex Binding Specificity Assays. Binding specificities of the anti-DNA quadruplex antibody for quadruplex DNAs relative to triplex and duplex DNAs were determined by competitive RIFB assays (C-RIFB). These assays were performed essentially as described above with minor modifications. Fifty picomoles of ^{32}P-end-labeled quadruplex samples, TET4, TG4, or G4, in TES buffer were incubated for 1 h at 37 °C with 50 μL tissue culture supernatant samples or 50 μL purified antibody samples containing 25 pmol of antibody. Unlabeled competitor DNAs (0−5 nmol) were added and TES buffer was added to a final volume of 100 μL. The reactions were incubated at 37 °C for 1 h and then transferred to individual wells of presoaked MultiScreen filtration plates and treated as described above.

Competition between native and denatured DNA quadruplexes for antibody binding was also studied by C-RIFB assays. Native end-labeled quadruplexes (50 pmol) were incubated with 25 pmol of antibody for 1 h, and then 0−5 nmol of unlabeled *native* or *denatured* DNA quadruplexes was added and the mixtures were incubated for an additional 1 h in a total volume of 100 μL at 37 °C. Denatured quadruplexes were prepared for immunoassays by diluting stock solutions in 0.1 mM Li_2EDTA (pH 7) and incubating at 100 °C for 1 h immediately prior to use. Antibody binding reactions were transferred to filter plates and processed as described above. Structures of all nucleic acids were verified by CD analyses *before* and *after radiolabeling* and *purification* to ensure the structural integrity of the intended competitors and labeled substrates. CD experiments were also used to verify that the quadruplex species had fully denatured to single strands in C-RIFB experiments that were intended to test IgG binding affinities of native and denatured quadruplexes (single strands).

RESULTS

Structural Characterization of DNA Substrates. Structures of each molecule used in this study were characterized by CD and NMR. Spectroscopic analyses were performed to ensure that molecules which were used in the immunochemical assays formed the desired structures. Figure 1 shows the sequences of these molecules and types of adopted structures. Quadruplexes (Figure 1A) were used to determine if the *me*$^{\nu}$IIB4 anti-DNA quadruplex antibody preparation was specific for quadruplexes. Our secondary goal was to determine to what extent triplex and duplex complexes bound to the antibody. While a hierarchy of binding affinities was found for the antibody by radioimmunofilter binding (RIFB) assays, quadruplexes were identified as preferential substrates.

In vitro studies with the oligonucleotide d(CGCG$_4$GCG) have shown that it forms a stable parallel-stranded tetramolecular quadruplex under ionic strength and pH conditions simulating those in the nucleus (*70*; B. A. Brown II, H. Li, and C. C. Hardin, unpublished results). Circular dichroism and one- and two-dimensional NMR experiments have

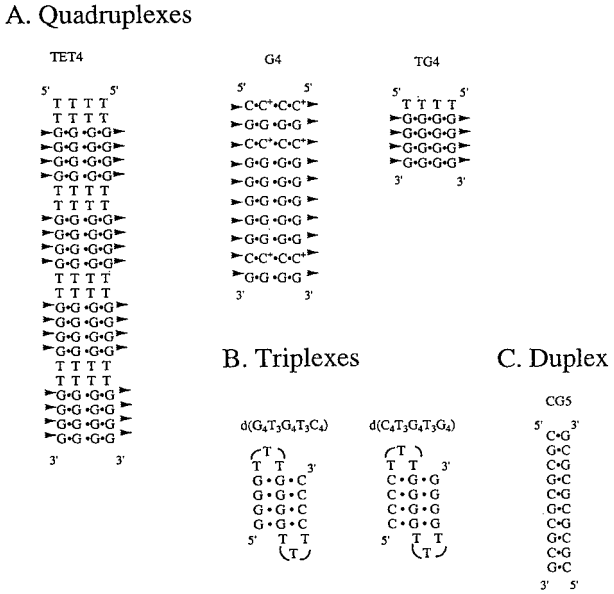

FIGURE 1: Nucleic acid structures used to assay the anti-DNA quadruplex antibody. Molecules are grouped according to the common structural motif: (A) quadruplexes, (B) intramolecular triplexes, (C) duplex formed from CG5 oligonucleotides. Arrows in quadruplexes indicate G•G base pairs between the four coplanar guanine residues, which cyclize the strands about the long axis by G-quartet formation.

shown that this quadruplex is very stable; the T_m is >95 °C in 10 mM NaH_2PO_4 (pH 7) and its stability persists in the presence of 50 mM KCl (results not shown). Gel electrophoresis studies have demonstrated that the complex remains intact in 10 mM KCl at pH 7 despite incubation at 100 °C for over 1 h (data not shown). This quadruplex denatures to single strands when incubated at 100 °C in 0.1 mM Li_2-EDTA (pH 7) for 30 min.

Thermodynamics and kinetics of quadruplex formation by the telomere-derived sequence d(TG$_4$) have been characterized in detail (*71*). This quadruplex is slightly less stable than the one formed by d(CGCG$_4$GCG) under equivalent conditions (T_m of ca. 85 °C in 10 mM NaH_2PO_4); the T_m increases to ≈95 °C upon addition of 50 mM KCl.

Quadruplex samples formed by the oligonucleotide d(T$_2$-G$_4$T$_2$G$_4$T$_2$G$_4$T$_2$G$_4$) were also tested (*60*). The parallel-stranded intermolecular quadruplex, TET4, has a T_m of approximately 85 °C in 10 mM NaH_2PO_4, pH 7, whereas the single-stranded intramolecular and folded-back hairpin bimolecular quadruplex species melt completely at ≈80 °C (*60*). The T_m of the intermolecular complex increases to about 95 °C when the complex is melted in 10 mM NaH_2-PO_4, pH 7, containing 50 mM KCl (results not shown).

Figure 2A shows CD data acquired in 10 mM NaH_2PO_4 buffer (pH 7) at 25 °C with labeled quadruplexes that were used in the RIFB and C-RIFB assays. Quadruplexes typically have maximum positive and negative ellipticities at ca. 264 and 240 nm, respectively. Upon melting, each of these bands decreases markedly. The parallel-stranded intermolecular quadruplex formed by four d(T$_2$G$_4$T$_2$G$_4$T$_2$-G$_4$T$_2$G$_4$) molecules has a maximum ellipticity at 262 nm. When the intermolecular TET4 quadruplex (≈7 μM) is melted in 10 mM NaH_2PO_4 containing 20 mM KCl, the denatured strands reanneal to form the same structure (results not shown), consistent with earlier studies which demon-

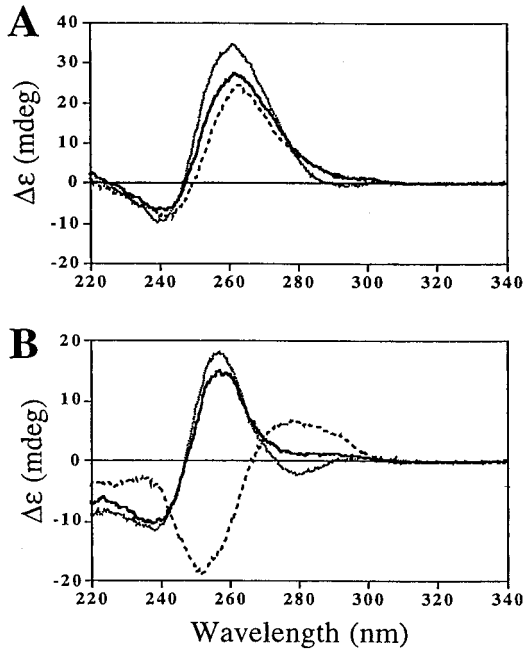

FIGURE 2: CD analyses of DNA samples to ensure formation of the anticipated structures. Samples were diluted from concentrated stock solutions to ca. 7 μM in 10 mM NaH_2PO_4 (pH 7), and spectra were acquired at 25 °C. (A) Quadruplexes: TET4 (heavy solid line); TG4 (light solid line); G4 (- - -). (B) Triplexes and duplex: d($G_4T_3G_4T_3C_4$) (heavy solid line); d($C_4T_3G_4T_3G_4$) (light solid line); CG5 (- - -).

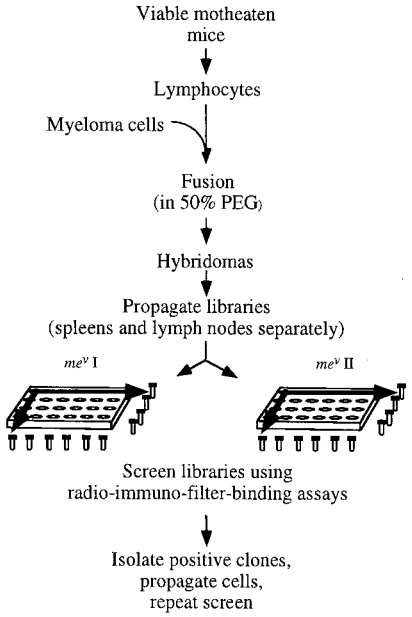

FIGURE 3: Viable motheaten library production. Hybridoma libraries were created from viable motheaten spleens and lymph nodes that were fused with myeloma cells. Lymph node-derived hybridomas were propagated separately from those derived from the spleens. Libraries were screened in a two-dimensional matrix to reduce the number of samples assayed. Positive "hits" on both the vertical and horizontal samples could be traced to individual wells. These cultures were expanded, rendered monoclonal, and rescreened for specificity.

strated that this sequence favors intermolecular quadruplex formation in the presence of K^+ (*60*).

Figure 2B shows CD spectra obtained with intramolecular triplex structures that are formed by the two oligos d($G_4T_3G_4T_3C_4$) and d($C_4T_3G_4T_3G_4$) in 10 mM NaH_2PO_4. These structures have characteristic spectra with maximum positive ellipticity at 257 nm and maximum negative ellipticity at 238 nm (*72*). The spectrum of d($C_4T_3G_4T_3G_4$) has an additional negative band at 279 nm that is not seen in d($G_4T_3G_4T_3C_4$) spectra. This negative band has been attributed to intramolecular G·G·C triplex formation in poly [d$(G)_2$·d(C)], which is dependent upon the presence of Mg^{2+} (*72*−*74*).

Melting temperatures of intramolecular triplexes formed by d($C_4T_3G_4T_3G_4$) and d($G_4T_3G_4T_3C_4$) are ca. 65 and 55 °C, respectively (results not shown), in agreement with Chen (*72*). The absence of negative ellipticity at 278 nm in the d($G_4T_3G_4T_3C_4$) spectrum and the lower T_m suggest that this oligonucleotide forms a triplex structure that is much less stable than that formed by d($C_4T_3G_4T_3G_4$).

Figure 2B also shows the CD spectrum of the B-form duplex DNA [d$(CGCGCGCG)_2$] (CG5). This spectrum is consistent with previously published results of B-DNA duplexes (*27*, *77*, *78*).

Detection and Purification of an Anti-DNA Quadruplex Antibody. A hybridoma that produces an autoantibody which preferentially binds DNA quadruplexes was isolated from a "fusion library" that was prepared using the cervical and mesenteric lymph nodes from two 3-month-old "viable motheaten" mice. This antibody will be referred to as "*me*^{v}-IIB4" (formerly called *me*^{v}-αQ_1; *79*). Serum from an 11-week-old motheaten mouse was screened for anti-quadruplex antibody binding activity in RIFB assays prior to obtaining mice for cell fusions. Low but reproducible levels of anti-quadruplex activity were detected in diluted serum, leading us to proceed with hybridoma experiments (data not shown).

Cervical and mesenteric lymph nodes from viable motheaten mice are very large and enriched with plasma cells. In contrast, viable motheaten spleens often contain significant numbers of atypical plasma cells and macrophages and have marked histopathological abnormalities (*80*−*82*). Spleens were not used for fusions because macrophages can quickly overgrow the resulting hybridoma cultures and thereby interfere with their proliferation.

Cells isolated from motheaten lymph nodes were fused with the BALB/c-derived P3 × 63Ag8.653 myeloma cells using poly(ethylene glycol) (1500) treatment. After fusion, cells were aliquotted into 24-well tissue culture plates for aminopterin selection and antigen screening. Figure 3 outlines the cloning and screening procedure. As a result of the low number of primary cells isolated from the cervical and mesenteric lymph nodes (ca. 5×10^5 cells/mouse), the hybridomas were not cloned by limiting dilution until after screening and expansion. In addition, feeder cells were not used to condition the hybridoma medium. Multiple colonies (between 6 and 10, sometimes as many as 15) were observed in each well. We estimate that the fused lymphocytes from two viable motheaten mice generated approximately 600−800 separate hybridomas. Cultures were initially screened for anti-quadruplex activity by ELISA as described (*31*, *37*). These assays were not precise enough for detecting anti-quadruplex antibodies, so cultures were screened by RIFB assays. This assay was a modification of the one used by Möller et al. (*31*). The RIFB assays provided a fast and reliable method with a sufficiently large signal-to-noise ratio to determine the specificity of the diluted antibody in tissue

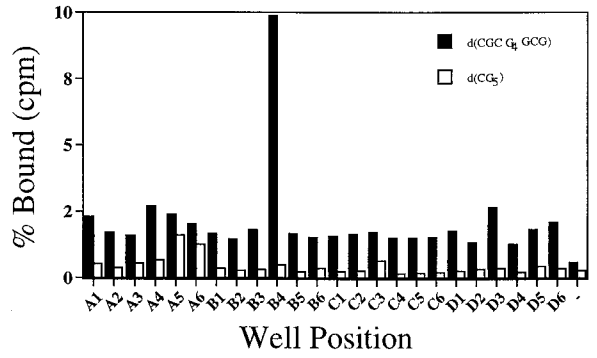

FIGURE 4: Hybridoma screening assay. Hybridomas were screened in RIFB assays after fusion using ^{32}P end-labeled G4 (■) and CG5 (□) as positive and negative substrates, respectively. Samples from well B4 were found to bind quadruplex with highest affinity and had minimal reactivity with the duplex. This culture was expanded and cloned by limiting dilution. Cultures A4 and D3 also had moderate anti-DNA quadruplex activity. Culture A5 was found to produce a general anti-DNA antibody. The dash indicates results for a negative control experiment performed with tissue culture medium.

culture supernatants. An important point is that RIFB assays provide information about the binding affinity of a DNA− or RNA−protein interaction without radically altering the structures of the DNA− or RNA−substrate complexes.

Anti-quadruplex antibodies were detected by assaying culture supernatants obtained from each well of the tissue culture plates with radiolabeled G4 in RIFB assays. The self-complementary intermolecular duplex [d(CGCGCGCGCG)$_2$], CG5, was used as a negative control to select against anti-G/C-rich duplex DNA antibodies. Figure 4 shows results of a representative RIFB assay of the hybridoma library from which the anti-DNA quadruplex antibody was isolated. During the initial screening of the motheaten fusion library, four cultures displayed anti-G4 binding activities above baseline levels (Figure 4). Three cultures (A4, B4, and D3) had anti-DNA quadruplex activities and low anti-double-stranded DNA activities. Culture B4 had anti-G4 binding affinity which was ca. 5-fold higher than the baseline level (Figure 4). This culture was expanded, rendered monoclonal by limited dilution culturing, and propagated for study. Culture A5 had approximately equal anti-double-stranded DNA and anti-quadruplex DNA affinities. The A4, A5, and D3 antibody cultures were also propagated, rendered monoclonal, and frozen for further analyses.

Antibodies were purified directly from tissue culture supernatants by T-Gel (Pierce) thiophilic-resin affinity chromatography (results not shown). This method was particularly useful because the antibody was concentrated and purified in a single-step procedure. Furthermore, the antibody was eluted from the column under very mild conditions (50 mM Tris·HCl, pH 8). Typical yields from the T-Gel columns were ≈0.5 mg/mL from about one liter of tissue culture supernatant processed. Purities of pooled column fractions were analyzed by SDS−PAGE (results not shown). Antibody fractions were found to be ≈95% homogeneous, with limited residual FBS contamination (from the tissue culture medium). The presence of residual FBS was taken into account when antibody concentrations were determined.

The *me^v*IIB4 antibody had an apparent molecular mass of ≈170 kDa based on gel-filtration chromatography and SDS−PAGE results. This molecular mass led us to believe that the antibody was an IgG (with typical molecular masses between 150 and 180 kDa, depending upon the extent of glycosylation). Results from ELISA experiments and Western blotting confirmed that the antibody heavy chain had the IgG3 isotype with κ light chains. These results were corroborated by PCR-based gene amplification analyses using primers corresponding to heavy- and light-chain immunoglobulin DNA sequences of IgM, IgG1, IgG2a, IgG2b, IgG3, and κ and λ light chains, which were supplied with the Ig-Prime kit (Novagen).

me^{v}IIB4 Antibody Binds Quadruplex DNAs with Higher Affinities Than Triplex and Duplex DNAs. Binding affinities of the *me^v*IIB4 antibody for quadruplex, triplex, and duplex DNA structures were determined by Scatchard and nonlinear regression analyses of RIFB isotherm data. These isothermal analyses were conducted at 37 °C for 2 h. Preliminary time-dependent binding assays demonstrated negligible increases in bound DNA concentrations after 2 h.

The Scatchard isotherm is constructed by plotting the number of moles of ligand bound per mole of binding site (fractional saturation, r) divided by the corresponding concentrations of unbound (free) ligand (r/C_{free}) (*67, 83−88*). In the simple linear case, the r intercept is the number of ligands bound. The slope of the line is equal to $-K_a$ and the r/C_{free} intercept is equal to nK_a. The Scatchard and nonlinear regression analyses initially assumed the following premises: (i) that the antigen (nucleic acid) binding sites on the antibody act independently (i.e., there is no linkage or cooperativity) and (ii) that a single epitope on the ligand (DNA) is bound by each antibody binding site. The association binding constant (K_a) determined for DNA binding to the antibody is a measurement of the *intrinsic affinity*, corresponding to *each of the antigen binding sites* treated in isolation.

Scatchard plots for the three quadruplexes used in these experiments are shown in Figure 5. Binding parameters obtained from the Scatchard analyses are listed in Table 1. The quadruplex TET4 had the highest affinity ($K_a = 2.28 \times 10^7$ M^{-1}), followed by G4 and then TG4, $K_a = 7.41 \times 10^6$ M^{-1} and $K_a = 5.95 \times 10^6$ M^{-1}, respectively. The triplex molecules d($G_4T_3G_4T_3C_4$) and d($C_4T_3G_4T_3G_4$) and the duplex CG5 all had similar affinities ($K_a = 7.86 \times 10^5$, 7.63×10^5, and 7.66×10^5 M^{-1}, respectively). From these results it appears that the antibody has at least a 10-fold higher affinity for quadruplexes than other DNA structures.

The Scatchard analysis is accurate and reliable when the interaction between ligand and binding site is *unimolecular* or the binding affinity of a site on a multisite "lattice" is unaffected by ligand binding to other sites (i.e., exhibits no cooperativity).

If ligand binding affects binding of subsequent ligands to adjacent sites, interpretation becomes more complicated. In the case of negative cooperativity, where ligand binding adversely influences binding of subsequent ligands, the Scatchard plot is hyperbolic with a concave upward shape. The curve will have a negative slope that approaches the r axis asymptotically. In the bimolecular binding-site case, a concave upward Scatchard plot can be decomposed into linear plots corresponding to two separate binding events (*83*, *89*, *90*); the first binding event has a stronger binding affinity than the second. The sum of the intercepts of the

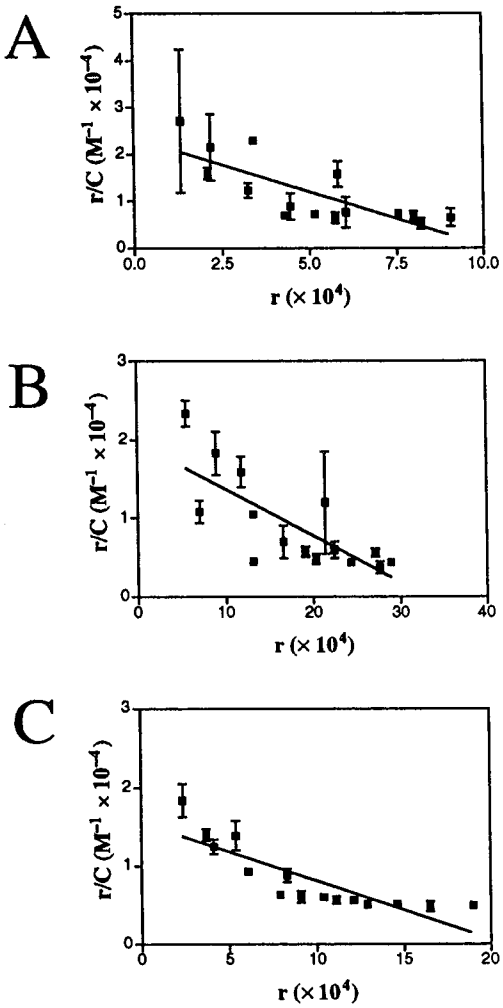

FIGURE 5: Scatchard plots of RIFB data for quadruplexes binding to the *me*^{v}IIB4 antibody. Binding parameters were derived from linear regression lines of Scatchard plots. (A) TET4; (B) TG4; (C) G4. Error bars correspond to the standard deviation of at least two experiments.

Table 1: Scatchard Binding Parameters Determined from Linear Regression Fits

molecule	K_a ($M^{-1} \times 10^{-5}$)	K_d[a] ($M \times 10^6$)	B_{max}[b] ($M \times 10^3$)	R^2
TET4[c]	228	0.044	1.03	0.601
TG4[c]	59.5	0.168	3.31	0.578
G4[c]	74.1	0.135	2.10	0.718
$d(G_4T_3G_4T_3C_4)$[d]	7.86	1.27	16.1	0.643
$d(C_4T_3G_4T_3G_4)$[d]	7.63	1.31	1.28	0.661
CG5[e]	7.66	1.31	4.84	0.934

[a] Calculated as $-1/K_a$. [b] B_{max} is equivalent to *n*, which is the molar concentration of ligand bound to individual Fab sites. [c] Quadruplex DNA. [d] Triplex DNA. [e] Duplex DNA.

two decomposed curves yields the concentration of ligands bound to the macromolecule.

In Scatchard plots, the *r* value is also used to calculate r/C_{free}, which violates the assumptions of linear regression, and thus the results of the regression are not strictly credible. As a result, nonlinear regression analysis of the untransformed binding data (r, C_{free}) in accordance with the appropriate binding expression (eq 5) is the preferred method for evaluating binding parameters (*68*, *69*, *91*, *92*).

Nonlinear Regression Analysis of [me^{v}*IIB4 IgG·(Q)*$_n$*] Binding Data.* Binding isotherms (r vs C_{free}) were analyzed

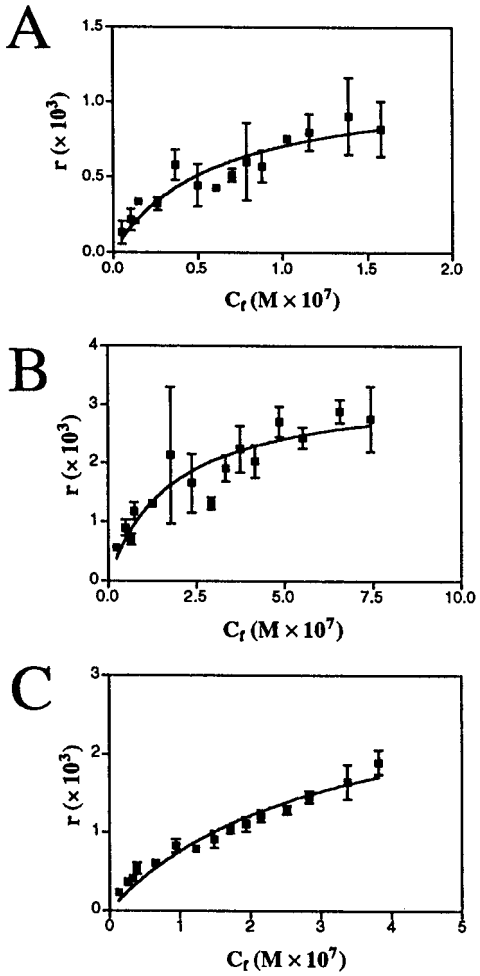

FIGURE 6: Binding isotherms for quadruplexes binding to the *me*^{v}-IIB4 antibody. Binding constants were obtained from nonlinear regression analyses of the binding isotherms. (A) TET4; (B) TG4; (C) G4. Error bars correspond to the standard deviation of at least two experiments.

Table 2: Binding Parameters Determined from Nonlinear Regression Fits

molecule	K_a ($M^{-1} \times 10^{-5}$)	K_d[a] ($M \times 10^6$)	B_{max}[b] ($M \times 10^3$)	R^2
TET4[d]	166	0.600	1.13	0.870
TG4[c]	53.8	0.186	3.31	0.840
G4[c]	33.0	0.303	3.07	0.948
$d(G_4T_3G_4T_3C_4)$[d]	6.76	1.48	18.6	0.886
$d(C_4T_3G_4T_3G_4)$[d]	5.59	1.79	13.9	0.885
CG5[e]	8.26	1.21	4.75	0.964

[a] Calculated as $-1/K_a$. [b] B_{max} is equivalent to *n*, which is the molar concentration of ligand bound to individual Fab sites. *c*Quadruplex DNA. *d*Triplex DNA. [e] Duplex DNA.

by nonlinear regression using the program PRISM (GraphPad Software, Inc.). Binding isotherms are shown in Figure 6 and results of the nonlinear analyses are displayed in Table 2. Consistent with results obtained by Scatchard analysis, quadruplexes were found to bind with at least 10-fold stronger affinities than the other DNA structures tested. TET4 had the highest affinity ($K_a = 1.66 \times 10^7$ M^{-1}), which was slightly lower than that obtained from Scatchard analysis. TG4 and G4 both had reduced affinities relative to those obtained by Scatchard analyses. Interestingly, TG4 had a slightly higher affinity than G4 (K_a values of 5.38×10^6 and 3.30×10^6 M^{-1}, respectively), the reverse of what was

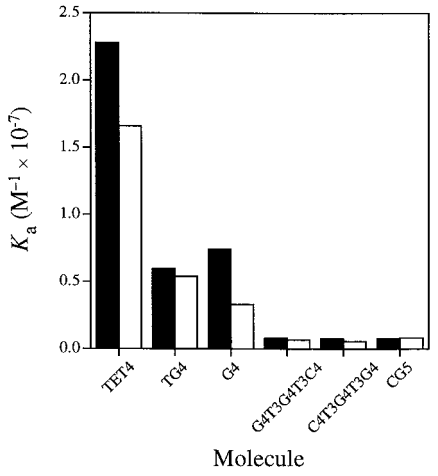

FIGURE 7: Comparison of binding affinities obtained by scatchard and nonlinear regression analyses. Scatchard-derived K_as (■) and nonlinear regression-derived K_as (□) are compared for each of the six molecules shown.

found by Scatchard analysis. Association binding constants (K_a) obtained by both Scatchard and nonlinear regression analyses are shown graphically in Figure 7.

The triplex molecules had binding constants similar to those seen with Scatchard analysis [d($G_4T_3G_4T_3C_4$) $K_a = 6.76 \times 10^5$ M^{-1} and d($C_4T_3G_4T_3G_4$) $K_a = 5.59 \times 10^5$ M^{-1}]. Surprisingly, CG5 had a slightly higher binding constant than both triplexes ($K_a = 8.26 \times 10^5$ M^{-1}), whereas binding was similar to that of the triplexes in the Scatchard analyses (Figure 7). This result could be due to the fact that the intermolecular triplexes have approximately four contiguous bases (in the triple helix) while CG5 has 10 bases involved in a duplex. This increased length could stabilize the duplex molecule in the antibody-combining site, whereas the triplexes may have fewer contacts with the antibody combining site, resulting in less stable complexes.

Interpretations of the [me^{v}IIB4 IgG·(Q)$_n$] Binding Data. The Scatchard data presented for binding of the three quadruplex (Q) molecules to *me^v*IIB4 IgG all have hyperbolic concave upward shapes, which is indicative of either two types of binding sites (as in polyclonal antisera) or negative cooperativity between two (or more) linked sites (*87*, *89*, *90*) (Figure 5). This complicates determination of the number of ligands bound to the antibody because the data approach the abscissa horizontally with nearly zero slope. One cannot determine the *r* intercept without performing biphasic decomposition analyses (*87*, *89*, *90*). The same data were plotted as (untransformed) *r* vs C_{free} isotherms and fit by nonlinear regression to determine K_a and *n* (Figure 6). However, the *n* values (B_{max}) were in the *millimolar* range, with K_as in the low to mid *micromolar* range. This inconsistency indicates that the binding events are more complicated than originally thought. The concave upward shapes of the curves in Figure 5 suggest that two sites bind quadruplexes per IgG and that the second ligand binds with negative cooperativity, $K_{a,2} < K_{a,1}$. Hill plots (data not shown) were constructed and slopes less than unity confirmed that these binding events were negatively cooperative. Two-site decomposition analyses were performed to determine binding parameters based upon the entire lattice, instead of treating each site in isolation. Analyses were performed using both linear (Scatchard) and nonlinear methods as described in Experimental Procedures. The binding association constants for the three quadruplex molecules tested were larger in both the Scatchard and nonlinear two-site binding cases (Tables 3 and 4). The first binding constants were larger than the second binding constants in all cases, demonstrating negative cooperativity.

Higher and lower affinity binding constants almost certainly represent the first and second Q-binding events, to the two complementary determining regions (CDRs) of the two Fab sites. The second occupied site should have a smaller microscopic association constant than the first ($K_{a,2} < K_{a,1}$) because one site is already occupied and the number of binding choices decreases from 2 to 1. Also, when one of the two sites is occupied by a quadruplex molecule, the [IgG·$(Q)_1$] complex is much less cationic than the antibody was prior to binding the first Q molecule.

Table 3: Binding Parameters Determined from Scatchard Analyses Using the Two-site Lattice Model

molecule	$K_{a,1}$[a] ($M^{-1} \times 10^{-6}$)	$B_{max,1}$[b] ($M \times 10^3$)	R^2	$K_{a,2}$[a] ($M^{-1} \times 10^{-6}$)	$B_{max,2}$[b] ($M \times 10^3$)	R^2
TET4[c]	24.4	2.10	0.348	2.08	7.88	0.212
TG4[c]	7.22	5.92	0.385	1.04	14.3	0.170
G4[c]	14.9	2.70	0.872	0.980	13.6	0.670
d($G_4T_3G_4T_3C_4$)[d]	12.4	7.69	0.637	1.64	22.6	0.849
d($C_4T_3G_4T_3G_4$)[d]	9.03	9.18	0.117	0.280	37.9	0.382
CG5[e]	0.485	14.3	0.743	0.343	13.0	0.377

[a] Calculated as the negative slope of the Scatchard plot. [b] B_{max} is equivalent to *n*, the molar concentration of ligand bound to individual Fab sites. [c] Quadruplex DNA. [d] Triplex DNA. [e] Duplex DNA.

Table 4: Binding Parameters Determined from Nonlinear Regression Fits Using the Two-Site Lattice Model

molecule	$K_{a,1}$ ($M^{-1} \times 10^7$)	$B_{max,1}$[a] ($M \times 10^3$)	$K_{a,2}$ ($M^{-1} \times 10^6$)	$B_{max,2}$[a] ($M \times 10^3$)	R^2
TET4[b]	0.299	1.21	0.176	1.28	0.880
TG4[b]	0.497	3.04	33.6	0.0136	0.874
G4[b]	0.103	0.776	4.59	0.375	0.990
d($G_4T_3G_4T_3C_4$)[c]	1.05	16.2	1.05	16.2	0.877
d($C_4T_3G_4T_3G_4$)[c]	1.08	6.28	0.28	9.10	0.962
CG5[d]	9.83	7.82	10.0	3.55	0.966

[a] B_{max} is equivalent to *n*, the molar concentration of ligand bound to individual Fab sites. [b] Quadruplex DNA. [c] Triplex DNA. [d] Duplex DNA.

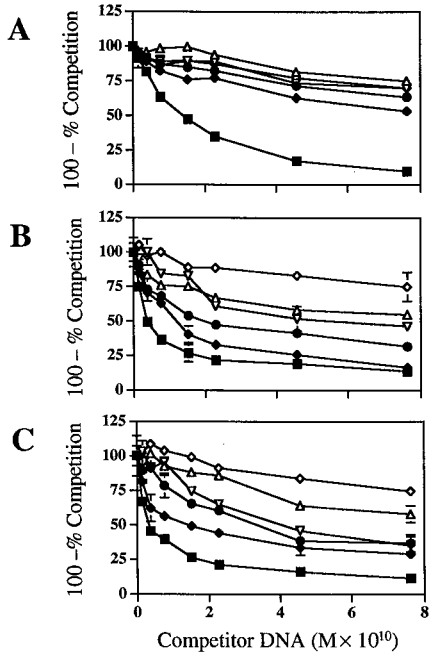

FIGURE 8: Competitive RIFB assays. Competitive filter-binding assays were performed by incubating 50 pmol of ^{32}P-end-labeled quadruplexes (A) TET4, (B) TG4, or (C) G4 with 25 pmol of purified anti-quadruplex antibody and the indicated amounts of unlabeled competitor nucleic acid complex (0−5 nmol). Error bars correspond to standard deviations of four determinations. Quadruplexes: (■) TET4; (◆) TG4, (●) G4. Triplexes: (△) d($G_4T_3G_4T_3C_4$), (▽) d($C_4T_3G_4T_3G_4$). Duplex: (◇) CG5.

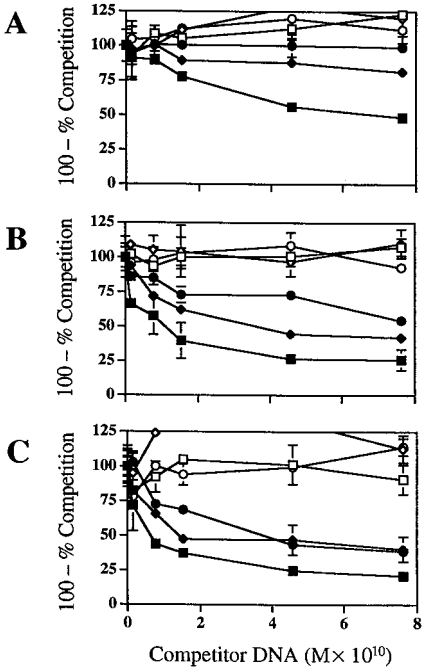

FIGURE 9: Competitive quadruplex C-RIFB assays. C-RIFB assays were performed with native or denatured quadruplexes by incubating 50 pmol of ^{32}P-end-labeled quadruplexes (A) TET4, (B) TG4, or (C) G4 with 25 pmol of purified anti-quadruplex antibody, and then competing with increasing amounts of unlabeled native or thermally denatured quadruplexes (0−5 nmol). Error bars correspond to standard deviations of four determinations. (■) Native TET4, (◆) native TG4, (●) native G4, (□) melted TET4, (◇) melted TG4, (○) melted G4.

Antibody Recognition Is Specific for Quadruplex DNAs. The capabilities of radiolabeled quadruplexes to compete with unlabeled quadruplex, triplex, and duplex competitors for antibody binding were assessed in competitive RIFB assays (C-RIFB). The results demonstrate that *me*$^{\nu}$IIB4 binds each of the quadruplexes in the presence of a 1000-fold molar excess of each unlabeled competitor DNA tested (Figure 8). Unlabeled quadruplexes were capable of competing with labeled quadruplexes for antibody binding in a manner consistent with the observed differences in binding affinities (Tables 1−4); the observed reduction in binding capacity was proportional to the amount of unlabeled homologous quadruplex DNA added. The TET4 quadruplex competed successfully with those formed by both TG4 and G4 (Figure 8A). In contrast, TG4 and G4 were not capable of effectively competing with TET4 for antibody binding (Figure 8B,C). Radiolabeled quadruplexes also bind preferentially relative to unlabeled triplex or duplex competitors (Figure 8), consistent with a ca. 10-fold or larger difference in K_a values (Tables 1−4).

Recognition of Quadruplex DNAs Is Dependent upon Conformation and Not Merely Sequence. Labeled DNA quadruplexes were incubated with *me*$^{\nu}$IIB4 and then assayed by C-RIFB to determine whether unlabeled native quadruplexes or thermally denatured strands could compete for antibody binding. The results in Figure 9A show that native unlabeled TET4 quadruplexes outcompete both TG4 and G4 for antibody binding, as evidenced by the loss of retained radioactivity at higher TET4 quadruplex concentrations. Unlabeled TG4 and G4 were also able to compete for binding with their respective labeled counterparts in homologous C-RIFB assays (Figure 9B,C). In contrast, thermally denatured quadruplexes (single strands) did not compete with native quadruplexes for *me*$^{\nu}$IIB4 binding. This indicates that the specificity of the anti-DNA quadruplex antibody depends not only upon base sequence or composition but also upon the overall conformation of the quadruplex. When denatured TG4 was added to binding assays containing labeled G4 or labeled TET4, the measured binding levels increased to slightly above 100% (≈110−120%) (Figure 9A,C), probably reflecting the overall uncertainty of the RIFB method.

DISCUSSION

Since the discovery of DNA quadruplexes, many questions have arisen regarding the biological relevance of these novel DNA structures (*4*, *16*). Possible biological roles and functions of quadruplexes have been speculated upon, but limited useful structural information has emerged from in vivo studies. This has been partly due to the lack of a reliable reagent to specifically detect quadruplexes in a complex biological preparation. The *me*$^{\nu}$IIB4 antibody reported here is the first immunoreagent we are aware of that reacts in a structurally specific manner with quadruplex DNAs. This should now allow attempts at reliable detection of quadruplexes and differentiation of quadruplexes from triplex and duplex structures.

In characterizing the specificity of this antibody, precautions were taken to verify the structural compatibility of the substrates, reagents, and assay conditions. CD spectra were acquired, after radiolabeling, purifying, and equilibrating the samples, to confirm the integrity of the chosen structure after manipulation under assay conditions. The antibody binds quadruplex structures with reasonable affinity and has

distinguishably lower cross-reactivities with other typical nucleic acid structures.

Traditionally, only antibodies expressing extremely high association constants ($K_a \approx 10^8-10^{10}$ M^{-1}) have been considered biologically important and useful for immunotechniques. Virtually without exception, such antibodies are the result of repeated immunizations and their variable regions have undergone somatic mutation to achieve these high affinities. In contrast, antibodies produced in the initial response to a variety of antigens have affinities in the micromolar range ($K_a \approx 10^5-10^7$ M^{-1}) (*93*). However, this affinity defines a demonstrable threshold ($\approx 10^5$ M^{-1}) for significant antibody−antigen interaction. In other words, affinities in this range are sufficient to induce B-cell proliferation and differentiation.

The autoantibody discussed here has affinities for different DNA structures above the 10^5 M^{-1} range. These results are consistent with the idea that anti-DNA antibodies do indeed undergo somatic mutation and affinity maturation to develop increased specificities (*94*). Sequencing data of the heavy- and light-chain variable regions has been compared to known viable motheaten anti-DNA antibodies (*95*, *96*). Both the heavy- and light-chain variable regions of the *me^v*IIB4 antibody have point mutations to the CDR3 region, which has been regarded as the major factor contributing to DNA binding (*97*).

Anti-DNA antibodies can be difficult to elicit because DNA is generally not particularly immunogenic (*98*−*100*). Prior to the work reported here, we attempted to use two methods to generate anti-quadruplex antibodies. Selections from mouse single-chain combinatorial immunoglobulin phage-display libraries (*101*) and classical DNA immunization/hybridoma fusion progeny were both unsuccessful routes to producing antibodies specific for the quadruplex structure. Bromination of the G4 quadruplex was attempted in order to increase its immunogenicity and specificity by emphasizing nonbackbone epitopes (*27*, *36*). While higher immunogenicity was achieved, these attempts were ineffective in generating increased anti-DNA quadruplex *structural* specificity.

Autoimmune, Immunodeficient Mice Produce a Quadruplex DNA Specific Antibody in Their "Normal" Repertoire. We purified *me^v*IIB4 directly from tissue culture media of monoclonal hybridomas produced from lymph nodes isolated from *unimmunized* mice by thiophilic T-Gel affinity chromatography (Pierce). The antibody was initially isotyped as an IgM, with κ light chains. This result is consistent with the finding that many anti-DNA autoantibodies from viable motheaten mice are IgMs (*80*, *81*, *96*). However, during the course of this investigation, our evidence indicates that the heavy chain gene in the hybridoma cell line underwent isotype switching to produce IgG3 antibodies. Isotype switching in vitro is not common but has been observed with a number of hybridoma lines (*64*). Further evidence for this phenomenon was obtained by using a PCR-based isotyping system (Ig-Prime, Novagen), in which genetic markers for both IgM and IgG heavy chains were detected concomitantly in cDNA libraries derived from mixed hybridoma cultures. The IgG3 anti-DNA quadruplex antibody has an apparent molecular mass of 1.7×10^5 Da based on gel-filtration chromatography and electrophoretic analyses.

An interesting point is that DNAs isolated from DNA−anti-DNA immune complexes from human lupus patients and NZB × NZW F_1 mice are usually rich in guanine−cytosine content (*51*, *58*). In addition, autoantibodies appear to preferentially select DNA sequences that are expected to form non-B-DNA structures (*47*). The latter observations may explain why we were able to successfully isolate an anti-G-DNA quadruplex antibody from an autoimmune mouse.

Several murine models of the autoimmune disease systemic lupus erythematosus readily produce anti-DNA antibodies (*102*, *103*). In this work, we isolated a naturally occurring anti-DNA quadruplex autoantibody from nonimmunized 3-month-old viable motheaten mice. These studies illustrate the general strategy of using autoimmune mice as a reservoir from which to acquire antibodies that recognize antigens which are not typically immunogenic or are very difficult to obtain.

Viable motheaten mice are severely immunodeficient with defects in both lymphoid and myeloid cell populations and, as a result, develop autoimmunity early in life (*81*). These mutant mice are named for the patchy absence of skin pigment which occurs as a result of neutrophilic accumulation in the dermis and epidermis and gives them a "motheaten" appearance. Homozygous motheaten mice have a mean life span of 9 weeks. Deleterious alleles at the motheaten locus on chromosome 6 result in the most severe immunological abnormalities known to result from point mutations (*104*). These mutations are within the structural gene encoding a cytoplasmic protein-tyrosine phosphatase, termed hematopoietic cell phosphatase (*104*). The molecular basis for the motheaten phenotype is due to aberrant splicing of *Hcph* mRNAs which encode at least two defective HCP proteins (*105*). The role of the HCP protein in hematopoiesis is implicated as a negative regulator of cellular proliferation and possibly cellular differentiation. Studies are underway to determine the mechanisms by which disruption of the *Hcph* gene causes the myriad of immunopathological abnormalities seen in the motheaten mutants (*104*).

Viable motheaten mice have polyclonal stimulated B-lymphocytes and develop hyperimmunoglobulinemia with multiple autoantibodies (*81*, *106*). The concentrations of IgM and IgG3 in sera are 50 and 20 times greater, respectively, than that of age-matched control animals (*106*). Autoantibodies are produced against many nuclear antigens. As a result of their autoimmune characteristics and polyclonal B-lymphocyte stimulation, viable motheaten mice have provided a successful route to generating anti-DNA quadruplex antibodies. Other autoantibodies that bind to unusual antigens have been obtained from unimmunized viable motheaten mice (*96*). Fusion libraries can be prepared easily and screened for various antigens and then frozen and stored for subsequent use. Our success in selecting anti-DNA quadruplex producing cells provides further evidence that this route may yield useful monoclonal antibodies when other methods fail.

Kee et al. (*107*) recently described the NAD^+-dependent binding of *Tetrahymena thermophila* dihydrolipoamide dehydrogenase (called TGP2) to quadruplex DNA. The K_d was 1.5×10^{-7} M, about 3-fold larger than found for *me^v*IIB4 IgG binding to TET4 ($K_d = 0.6 \times 10^{-7}$ M); the affinity of *me^v*IIB4 IgG for TET4 is about 3-fold higher than that of

TGP2 for quadruplex DNA. While both interactions are suggestive and provide "a basis for continued experimentation, definitive demonstration of the existence and role of G4 (quadruplex), DNA in vivo remains an elusive goal" (*107*). The use of *me*^{v}IIB4 IgG and a "single-chain antibody" derived from it, which retains quadruplex DNA specificity (*95*), are currently being applied in pursuit of this goal. Sequence analysis (*95*) demonstrates homologies between the antibody complementarity determining regions and sequences from Myb family telomere binding proteins, which are hypothesized to control cell aging via telomeric DNA interactions. The presence of this antibody in the autoimmune repertoire suggests a possible linkage between autoimmunity, telomeric DNA binding proteins, and aging.

ACKNOWLEDGMENT

We thank Drs. Elizabeth Reap and Phil Cohen (Department of Rheumatology, University of North Carolina, Chapel Hill, NC) for providing the MRL/Mp-*lpr*/*lpr* anti-DNA sera, Jeff Kuhn for experimental assistance, and Matthew Corregan and David Lieberman for critical review of the manuscript and assistance with CD data processing. We also thank Professors Paul Agris and Stuart Maxwell (Department of Biochemistry, North Carolina State University, Raleigh, NC), Dr. Alan Herbert, Professor Alexander Rich (Department of Biology, MIT, Cambridge, MA), and Professor David Stollar (Tufts University, Boston, MA) for helpful discussions.

REFERENCES

1. Henderson, E. R., and Larson, D. D. (1991) *Curr. Opin. Struct. Biol. 1*, 538−543.
2. Sundquist, W. I. (1993) *Curr. Opin. Struct. Biol. 3*, 893−895.
3. Williamson, J. R. (1993) *Curr. Opin. Struct. Biol. 3*, 357−362.
4. Williamson, J. R. (1994) *Annu. Rev. Biophys. Biomol. Struct. 23*, 703−730.
5. Hardin, C. C., Corregan, M. J., Brown, B. A., II, and Frederick, L. (1993) *Biochemistry 32*, 5870−5880.
6. Henderson, E. R, Hardin, C. C., Wolk, S. K., Tinoco, I., Jr., and Blackburn, E. H. (1987) *Cell 51*, 899−908.
7. Sen, D., and Gilbert, W. (1988) *Nature 334*, 364−366.
8. Sen, D., and Gilbert, W. (1992) *Methods Enzymol. 211*, 191−199.
9. Pluta, A. T., and Zakian, V. A. (1989) *Nature 337*, 429−433.
10. Blackburn, E. H. (1990) *J. Biol. Chem. 265*, 5919−5921.
11. Williamson, J. R., Raghuraman, M. K., and Cech, T. R. (1989) *Cell 59*, 871−880.
12. Gottschling, D. A, Aparicio, O. M., Billington, B. L., and Zakian, V. A. (1990) *Cell 63*, 751−762.
13. Raghuraman, M. K., and Cech, T. R. (1990) *Nucleic Acids Res. 18*, 4543−4552.
14. Zahler, A. M., Williamson, J. R., Cech, T. R., and Prescott, D. M. (1991) *Nature 350*, 718−720.
15. Kipling, D. (1995) in *The Telomere*, pp 59−77, Oxford University Press, New York.
16. Zakian, V. A. (1995) *Science 270*, 1601−1607.
17. Abdul-Manan, N., O'Malley, S. M., and Williams, K. R. (1996) *Biochemistry 35*, 3545−3554.
18. Fry, M., and Loeb, L. A. (1994) *Proc. Natl. Acad. Sci. U.S.A. 91*, 4950−4954.
19. Briggs, M. R., Kadonaga, J. T., Bell, S. P., and Tjian, R. (1986) *Science 234*, 47−52.
20. Smith, S. S., Baker, D. J., and Jardines, L. A. (1989) *Biochem. Biophys. Res. Commun. 160*, 1397−1402.
21. Conrad, M. N., Wright, J. H., Wolf, A. J., and Zakian, V. A. (1990) *Cell 63*, 739−750.
22. Walsh, K., and Gualberto, A. (1992) *J. Biol. Chem. 267*, 13714−13718.
23. Kuwahara, J., Yonezawa, A., Futamura, M., and Sugiura, Y. (1993) *Biochemistry 32*, 5994−6001.
24. Giraldo, R., and Rhodes, D. (1994) *EMBO J. 13*, 2411−2420.
25. Weisman-Shomer, P., and Fry, M. (1993) *J. Biol. Chem. 268*, 3306−33112.
26. Johnston, M. I., and Stollar, B. D. (1978) *Biochemistry 17*, 1959−1964.
27. Lafer, E. M., Möller, A., Nordheim, A., Stollar, B. D., and Rich, A. (1981) *Proc. Natl. Acad. Sci. U.S.A. 78*, 3546−3550.
28. Lafer, E. M., Valle, R. P., Möller, A., Nordheim, A., Schur, P. H., Rich, A., and Stollar, B. D. (1983) *J. Clin. Invest. 71*, 314−321.
29. Nordheim, A., Pardue, M. L., Lafer, E. M., Möller, A., Stollar, B. D., and Rich, A. (1981) *Nature 294*, 417−422.
30. Nordheim, A., Herrera, T. E., and Rich, A. (1987) *Nucleic Acids Res. 15*, 1661−1677.
31. Möller, A., Gabriels, J. E., Lafer, E. M., Nordheim, A., Rich, A., and Stollar, B. D. (1982) *J. Biol. Chem. 257*, 12081−12085.
32. Möller, A., Nordheim, A., Kozlowski, S. A., Patel, D. J., and Rich, A. (1984) *Biochemistry 23*, 54−62.
33. Ballard, D. W., Lynn, S. P., Gardner, J. F., and Voss, E. W., Jr. (1984) *J. Biol. Chem. 259*, 3492−3498.
34. Arndt-Jovin, D. J., Robert-Nicoud, M., Baurschmidt, P., and Jovin, T. (1985) *J. Cell Biol. 101*, 1422−1433.
35. Braun, R. P., and Lee, J. S. (1986) *Nucleic Acids Res. 14*, 5049−5065.
36. Hardin, C. C., Zarling, D. A., Puglisi, J. D., Trulson, M. O., Davis, P. W., and Tinoco, I., Jr. (1987) *Biochemistry 26*, 5191−5199.
37. Hardin, C. C., Zarling, D. A., Wolk, S. K., Ross, W. S., and Tinoco, I., Jr. (1988) *Biochemistry 27*, 4169−4177.
38. Lee, J. S., Burkholder, G. D., Latimer, L. P., Haug, B. L., and Braun, R. P. (1987) *Nucleic Acids Res. 15*, 1047−1061.
39. Sheer, U., Messner, K., Hazan, R., Raska, I., Hansmann, P., Falk, H., Speiss, E., and Franke, W. W. (1987) *Eur. J. Cell Biol. 43*, 358−371.
40. Zarling, D. A., Calhoun, C. J., Hardin, C. C., and Zarling, A. H. (1987) *Proc. Natl. Acad. Sci. U.S.A. 84*, 6117−6121.
41. Zarling, D. A., Deikmann, S., and Calhoun, C. J. (1989) *Struct. Expression 3*, 87−96.
42. Zarling, D. A., Calhoun, C. J., Feuerstein, B. G., and Sena, E. P. (1990) *J. Mol. Biol. 211*, 147−160.
43. Burkholder, G. D., Latimer, L. J. P., and Lee, J. S. (1988) *Chromosoma 9*, 185−192.
44. Sanford, D. G., Kotkow, K. J., and Stollar, B. D. (1988) *Nucleic Acids Res. 16*, 10643−10655.
45. Wittig, B., Dorbic, T., and Rich, A. (1991) *Proc. Natl. Acad. Sci. U.S.A. 88*, 4350−4354.
46. Stollar, B. D (1992) *Prog. Nucleic Acids Res. Mol. Biol. 42*, 39−77.
47. Herrmann, M., Winkler, T. H., Fehr, H., and Kalden, J. R. (1995) *Eur. J. Immunol. 25*, 1897−1904.
48. Diekman, S., and Zarling D. A. (1987) *Nucleic Acids Res. 15*, 6063−6075.
49. Andrzejewski, C., Jr., Stollar, B. D., Lalor, T. M., and Schwartz, R. S. (1980) *J. Immunol. 124*, 1499−1502.
50. Eliat, D., Asofsky, R., and Laskov, R. (1980) *J. Immunol. 124*, 766−768.
51. Eliat, D., Hochberg, M., Fischel, R., and Laskov, R. (1982) *Proc. Natl. Acad. Sci. U.S.A. 79*, 3818−3822.
52. Tron, F., Charron, D., Bach, J.-F., and Talal, N. (1980) *J. Immunol. 125*, 2805−2809.
53. Lee, J. S., Lewis, J. R., Morgan, A. R., Mosmann, T. R., and Singh, B. (1981) *Nucleic Acids Res. 9*, 1707−1721.
54. Ballard, D. W., and Voss, E. W. (1982) *Mol. Immunol. 19*, 793−799.
55. Munns, T. W., Liszewskie, M. K., Tellam, J. T., Ebling, F. M., and Hahn, B. H. (1982) *Biochemistry 21*, 2929−2936.
56. Kardost, R. R. P., Billing, P. A., and Voss, E. W. (1982) *Mol. Immunol. 19*, 963−962.
57. Pistesky, D. S., and Caster, S. A. (1982) *Mol. Immunol. 19*, 645−650.

58. Sano, H., and Morimoto, C. (1982) *J. Immunol. 128*, 1341−1345.
59. Madaio, M. P., Hodder, S., Schwartz, R. S., and Stollar, B. D. (1984) *J. Immunol. 132*, 872−876.
60. Hardin, C. C., Henderson, E., Watson, T., and Prosser, J. (1991) *Biochemistry 30*, 4460−4472.
61. Hardin, C. C., Watson, T., Corregan, M. J., and Bailey, C. (1992) *Biochemistry 31*, 833−841.
62. Otting, G., Grutter, R., Leupin, W., Minganti, C., Ganesh, K. N., Sproat, B. S., Gait, M. J., and Wuthrich, K. (1987) *Eur. J. Biochem. 166*, 215−220.
63. Oi, V. T., and Herzenberg, L. A. (1980) Immunoglobulin-producing hybrid cells lines, in *Selected Methods in Cellular Immunology* (Mishell, B. B., and Shiigi, S. M., Eds.) pp 351−372, W. H. Freeman Co., San Francisco, CA.
64. Harlow, E., and Lane, D. (1988) in *Antibodies: A Laboratory Manual*, pp 553−612, Cold Spring Harbor Laboratory, Cold Spring Harbor, NY.
65. Towbin, H., Staehelin, T., and Gordon, J. (1979) *Proc. Natl. Acad. Sci. U.S.A. 76*, 4350−4354.
66. Zouali, M., and Stollar, B. D. (1986) *J. Immunol. Methods 90*, 105−110.
67. Scatchard, G. (1949) *Ann. N.Y. Acad. Sci. 51*, 660−672.
68. Moltulsky, H. J. (1995) *Prism 2.0 User's Guide*, pp 303−317, GraphPad Software, Inc., San Diego, CA.
69. Motulsky, H. (1996) *The Graphpad Guide To Analyzing Radioligand Binding Data*, pp 2−8, GraphPad Software Inc., San Diego, CA.
70. Goodlett, D. R., Camp, D. G., II, Hardin, C. C., Corregan, M. J., and Smith, R. D. (1993) *Biol. Mass Spectrom. 22*, 181−183.
71. Hardin, C. C., Corregan, M. J., Lieberman, D. V., and Brown, B. A., II (1997) *Biochemistry 36*, 15428−15450.
72. Chen, F.-M. (1991) *Biochemistry 30*, 4472−4479.
73. Marck, C., and Theile, D. (1978) *Nucleic Acids Res. 5*, 1017−1028.
74. Theile, D., Marck, C., Schneider, C., and Guschlbauer, W. (1978) *Nucleic Acids Res. 5*, 1997−2012.
75. Olivas, W. M., and Maher, L. J., III (1995) *Biochemistry 34*, 278−284.
76. Olivas, W. M., and Maher, L. J., III (1995) *Nucleic Acids Res. 23*, 1936−1941.
77. Uesugi, S., Ohkubo, M., Urata, H., Ikehara, M., Kobayashi, Y., and Kyogoko, Y. (1984) *J. Am. Chem. Soc. 106*, 365−3676.
78. Wolk, S., Thurmes, W. N., Ross, W. S., Hardin, C. C., and Tinoco, I., Jr. (1989) *Biochemistry 28*, 2452−2459.
79. Brown, B. A., II, Li, Y., Roberts, J. F., and Hardin, C. C. (1995) *Nucleic Acids Symp. Ser. 33*, 134−136.
80. Green, M. C., and Shultz, L. D. (1975) *J. Hered. 66*, 250−258.
81. Shultz, L. D. (1988) *Curr. Top. Microbiol. Immunol. 137*, 216−222.
82. Schweitzer, P. A., Taylor, S. E., and Shultz, L. D. (1991) *J. Cell Biol. 114*, 35−43.
83. Klotz, I. M., and Hunston, D. L. (1971) *Biochemistry 10*, 3065−3069.
84. McGhee, J. D., and von Hippel, P. H. (1974) *J. Mol. Biol. 86*, 469−489.
85. Chamness, G. C., and McGuire, W. L. (1975) *Steroids 2*, 538−542.
86. Klotz, I. M. (1982) *Science 217*, 1247−1249.
87. Berzofsky, J. A., Epstein, S. L., and Berkower, I. J. (1989) in *Fundamental Immunology*, 2nd ed. (Paul, W. E., Ed.) pp 315−356, Raven Press Ltd., New York.
88. Wyman, J., and Gill, S. (1989) in *Binding and Linkage*, University Science Books, Mill Valley, CA.
89. Schreier, A. A., and Shimmel, P. R. (1973) *J. Mol. Biol. 86*, 601−620.
90. Cantor, C. R., and Schimmel, P. R. (1980) in *Biophysical Chemistry Part III*, pp 849−886, W. H. Freeman and Co., New York.
91. Klotz, I. M. (1983) *Science 220*, 981−983.
92. Winzor, D. J., and Sawyer, W. H. (1995) in *Quantitative Characterization of Ligand Binding*, pp 1−11, Wiley-Liss, New York.
93. Kelsoe, G. (1992) in *Molecular Immunobiology of Self-Reactivity* (Bona, C. A., and Kaushik, A. K., Eds.) pp 81−92, Marcel Dekker, Inc., New York.
94. Shlomchik, M., Mascelli, M., Shan, H., Radic, M. Z., Pisetsky, D., Marshak-Rothstein, A., and Weigert, M. (1990) *J. Exp. Med. 171*, 265−292.
95. Brown, J., Brown, B. A., II, Li, Y., and Hardin, C. C. (1998) *Biochemistry 37*, xxxxx−xxxxx.
96. Westhoff, C. M., Whittier, A., Kathol, S., McHugh, J., Zajicek, C., Schultz, L. D., and Wylie, D. E. (1997) *J. Immunol. 159*, 3024−3033.
97. Radic, M. Z., Mackel, J., Erikson, J., Mol., C., Anderson, W. F., and Weigert, M. (1993) *J. Immunol. 150*, 4966−4977.
98. Stollar, B. D. (1980) *Methods in Enzymol. 70*, 71−85.
99. Stollar, B. D. (1980) *CRC Crit. Rev. Biochem. 2*, 1−36.
100. Schwartz, R. S., and Stollar, B. D. (1985) *J. Clin. Invest. 75*, 321−327.
101. Marks, J. D., Hoogenboom, H. R., Griffiths, A. D., and Winter, G. (1992) *J. Biol. Chem. 267*, 16007−16010.
102. Theofilopoulos, A. N., and Dixon, F. J. (1985) *Adv. Immunol. 37*, 269−390.
103. Shultz, L. D., and Sidman, C. L. (1987) *Annu. Rev. Immunol. 5*, 367−403.
104. Shultz, L. D., Schweitzer, P. A., Rajan, T. V., Yi, T. Ihle, J. N., Matthews, R. J., Thomas, M. L., and Beir, D. R. (1993) *Cell 73*, 1445−1454.
105. Tsui, F. W. L., and Tsui, H. W. (1994) *Immunol. Rev. 138*, 185−206.
106. Shultz, L. D., and Green, M. C. (1976) *J. Immunol. 116*, 936−943.
107. Kee, K., Niu, L., and Henderson, E. (1998) *Biochemistry 37*, 4224−4234.

BI981354U